

Side-band Inequivalence: The Unexpected Symmetry Breaking

Sina Khorasani*

(Dated: November 16, 2018)

In this letter, the recently predicted Side-band Inequivalence in quantum optomechanics, which is used to refer to the unequal shifts in blue and red-scattered photons, is analyzed to the full order. The mathematical method employed here is a combination of operator algebra equipped with harmonic balance, which allows a clear understanding of the associated nonlinear process. This reveals the existence of three distinct operation regimes in terms of pump power or intracavity photon number, two of which have immeasurably small side-band inequivalence. It is shown that the maximum attainable side-band inequivalence may be expected at an optimal operation point.

The nonlinearity of optomechanical interaction [1–9] causes scattering of incident photons with the annihilator \hat{a} from the cavity unto either red- or blue-shifted photons through annihilation or generation of a cavity phonon with the annihilator \hat{b} , giving rise to the first-order mechanical side-bands. Taking the optical frequency ω to be at a detuning $\Delta = \omega_c - \omega$ from cavity resonance ω_c , the ν -th order sidebands are naturally expected to occur at the detunings $\Delta_{\pm\nu} = \Delta \mp \nu\Omega$, where Ω represents the mechanical frequency. As a results, the first-order mechanical side-bands of scattered red Δ_{+1} and blue Δ_{-1} processes must average out back to the original pump detuning Δ .

Defining the side-band inequivalence as the deviation of this average from Δ , as $\delta = \frac{1}{2}(\Delta_{+1} + \Delta_{-1}) - \Delta$, then one may conclude $\delta = 0$. A non-zero δ would have otherwise implied the so-called Side-band Inequivalence. This type asymmetry appears to have a classical nonlinear nature.

There is, however, another well-known type of side-band asymmetry between the red and blue side-bands in the context of optomechanics, which has a quantum nature and may be used for instance to accurately determine the absolute temperature through a reference-free optomechanical measurement [10, 11]. This is based on the ratio of Stokes to anti-Stokes Raman transition rates, which is equal to $\exp(\hbar\Omega/k_B T)$ where k_B is the Boltzmann's constant and T is the absolute temperature [12, 13]. Clearly, side-band inequivalence is quite different from this type of side-band asymmetry.

While both time-reversal symmetry and energy conservation are fundamentally preserved in this scattering process, a nonlinear analysis of quantum optomechanics using the recently developed method of higher-order operators [14–17] necessitates a slight difference among detunings of blue and red-scattered photons, the amount of which was initially found to increase roughly proportional to the intracavity photon number \bar{n} . Here, \bar{n} is defined as the steady-state mean-value of the number operator $\hat{n} = \hat{a}^\dagger \hat{a}$.

Surprisingly enough, this disagreement satisfying $\delta \neq 0$ does not violate the energy conservation law, actually allowed by the finite cavity linewidth as well as the single-photon/single-phonon nature of the process involved.

Moreover, the time-reversal symmetry is also preserved.

Among the pool of available experimental data, only a handful of side-band resolved cavities reveal this disagreement [14]. Some initial trial experiments recently done at extremely high intracavity photon numbers \bar{n} , and/or extremely large single-photon optomechanical interaction rates g_0 , though, failed to demonstrate its existence. This may raise the speculation that whether side-band inequivalence would have been merely a mathematical artifact, or something has been missing due to not doing the operator analysis to the highest-order.

A careful analysis of this phenomenon, however, confirms the latter, thus classifying the quantum optomechanical interaction into three distinct regimes with different behaviors:

- **Fully Linear:** This regime can be investigated using the lowest-order analysis and first-order operators, which is conventionally done by linearizing the Hamiltonian around equilibrium points. This will require the four-dimensional basis of first-order ladder operators $\{\hat{a}, \hat{a}^\dagger, \hat{b}, \hat{b}^\dagger\}$ and is indeed quite sufficient to understand many of the complex quantum optomechanical phenomena [18].
- **Weakly Nonlinear:** This regime requires higher-order operator analysis of at least second-order. This can be done using the three-dimensional reduced basis [14, 18] given as $\{\hat{a}, \hat{a}\hat{b}, \hat{a}\hat{b}^\dagger\}$.
- **Strongly Nonlinear:** Full understanding of this interaction regime requires the highest-order analysis using third-order operators. Referred as to the minimal basis [14, 18], the convenient reduced choice is the two-dimensional basis $\{\hat{n}^2, \hat{n}\hat{b}\}$. While most of the quantum optomechanical experiments happen to fall in this regime, the striking behavior of governing equations is in such a way that a fully-linearized analysis of fluctuations mostly happens to work.

Side-band Inequivalence is essentially forbidden in the fully linear regime, and it also quickly fades away in the strongly nonlinear regime. But it may only happen in the weakly nonlinear regime. This is now also confirmed both by the higher-order operator method and extensive calculations. It typically does not exceed one part in

million to one part in ten thousand, and therefore, it is a very delicate phenomenon and elusive to observe.

This letter provides a direct route towards clear understanding of this complex nonlinear phenomenon. Using a combination of operator algebra and harmonic balance (used in analysis of laser diodes) [19], we obtain a closed form expression for side-band inequivalence δ as a function of intracavity photon number \bar{n} , which is expected to be valid through all three above operation regimes, and for any arbitrarily chosen set of optomechanical parameters. It can be shown that there is an optimal point at which the side-band inequivalence attains a maximum. Moving away from the optimal point, both at the much smaller and much larger pump rates, δ attains much smaller values, tending to zero in the limit of very large \bar{n} .

This will be greatly helpful to designate the investigation range of experimental parameters given any available optomechanical cavity. Furthermore, it marks a clear and definable border among the three above-mentioned operation regimes.

The analysis of side-band inequivalence proceeds with considering the behavior of optomechanical cavity under steady-state conditions. We will focus only on the first-order side-bands and discard all other contributions coming from or to the second- and higher-order side-bands. We consider a single-frequency pump with ideally zero linewidth at a given detuning Δ , which normally gives rise to two stable blue- and red- side-bands. Hence, the time-dependence of the photon annihilator will look like

$$\hat{a}(t) = \hat{a}_0 e^{i\Delta t} + \hat{a}_b e^{i(\Delta - \Omega + \frac{1}{2}\delta)t} + \hat{a}_r e^{i(\Delta + \Omega + \frac{1}{2}\delta)t} + \dots, \quad (1)$$

where \hat{a}_0 , \hat{a}_b , and \hat{a}_r respectively correspond to the central excitation resonance at pump frequency, and blue- and red-detuned side-bands. The steady-state time-average of central excitation satisfies $\langle \hat{a}_0 \rangle = \sqrt{\bar{n}}$, where \bar{n} can be determined by solution of a third-order algebraic equation once the optical power pump rate P_{op} , detuning Δ , external coupling η and all other optomechanical parameters are known. The standard set of basic optomechanical parameters needed here are mechanical frequency Ω , optical decay rate κ , and mechanical decay rate Γ . Therefore, the photon number operator will behave as

$$\begin{aligned} \hat{n}(t) = & \hat{a}_0^\dagger \hat{a}_0 + \hat{a}_b^\dagger \hat{a}_b + \hat{a}_r^\dagger \hat{a}_r \\ & + \hat{a}_b^\dagger \hat{a}_0 e^{i(-\Omega + \frac{1}{2}\delta)t} + \hat{a}_0 \hat{a}_b^\dagger e^{-i(-\Omega + \frac{1}{2}\delta)t} + \\ & + \hat{a}_r^\dagger \hat{a}_0 e^{i(\Omega + \frac{1}{2}\delta)t} + \hat{a}_0 \hat{a}_r^\dagger e^{-i(\Omega + \frac{1}{2}\delta)t} + \dots, \end{aligned} \quad (2)$$

while the mechanical annihilator will exhibit a closely spaced doublet around the mechanical frequency spaced within δ as

$$\hat{b}(t) = \hat{b}_0 + \hat{b}_b e^{-i(\Omega - \frac{1}{2}\delta)t} + \hat{b}_r e^{-i(\Omega + \frac{1}{2}\delta)t} + \dots. \quad (3)$$

Here, the average mechanical displacement satisfies

$$b_0 = \langle \hat{b}_0 \rangle = \frac{ig_0 \bar{n}}{i\Omega + \frac{1}{2}\Gamma}. \quad (4)$$

Now, let us get back to the Langevin equation for mechanical motions, which simply is

$$\frac{d}{dt} \hat{b}(t) = (-i\Omega - \frac{1}{2}\Gamma) \hat{b}(t) + ig_0 \hat{n}(t) + \sqrt{\Gamma} \hat{b}_{\text{in}}(t), \quad (5)$$

where $\hat{b}_{\text{in}}(t)$ is the operator for mechanical fluctuations. For the purpose of our analysis here, all fluctuations can be discarded since they are irrelevant to the formation of side-band frequencies and average out to zero. Using (2) and (3) we get

$$\begin{aligned} & -i(\Omega + \frac{\delta}{2}) \hat{b}_r e^{-i(\Omega + \frac{\delta}{2})t} - i(\Omega - \frac{\delta}{2}) \hat{b}_b - b e^{-i(\Omega - \frac{\delta}{2})t} \\ & \approx -(i\Omega + \frac{\Gamma}{2}) \hat{b}_r e^{-i(\Omega + \frac{\delta}{2})t} - (i\Omega + \frac{\Gamma}{2}) \hat{b}_b e^{-i(\Omega - \frac{\delta}{2})t} \\ & + ig_0 \hat{a}_0 \hat{a}_b e^{-i(\Omega - \frac{\delta}{2})t} + ig_0 \hat{a}_r^\dagger \hat{a}_0 e^{-i(\Omega + \frac{\delta}{2})t} + \dots \end{aligned} \quad (6)$$

From the above, we obtain two key operator equations

$$\begin{aligned} \hat{b}_r &= \frac{i2g_0}{-i\delta + \Gamma} \hat{a}_r^\dagger \hat{a}_0, \\ \hat{b}_b &= \frac{i2g_0}{i\delta + \Gamma} \hat{a}_0 \hat{a}_b. \end{aligned} \quad (7)$$

In a similar manner, the Langevin equation for the photon annihilator is

$$\frac{d}{dt} \hat{a}(t) = (i\Delta - \frac{1}{2}\kappa) \hat{a}(t) + ig_0 \hat{a}(t) [\hat{b}(t) + \hat{b}^\dagger(t)] + \sqrt{\kappa} \hat{a}_{\text{in}}. \quad (8)$$

Using (1) and (3) we obtain

$$\begin{aligned} & i\Delta \hat{a}_0 e^{i\Delta t} + i(\Delta - \Omega + \frac{\delta}{2}) \hat{a}_b e^{i(\Delta - \Omega + \frac{\delta}{2})t} \\ & + i(\Delta + \Omega + \frac{\delta}{2}) \hat{a}_r e^{i(\Delta + \Omega + \frac{\delta}{2})t} \approx \\ & (i\Delta - \frac{\kappa}{2}) \left[\hat{a}_0 e^{i\Delta t} + \hat{a}_b e^{i(\Delta - \Omega + \frac{\delta}{2})t} + \hat{a}_r e^{i(\Delta + \Omega + \frac{\delta}{2})t} \right] \\ & + ig_0 \left[\hat{a}_0 e^{i\Delta t} + \hat{a}_b e^{i(\Delta - \Omega + \frac{\delta}{2})t} + \hat{a}_r e^{i(\Delta + \Omega + \frac{\delta}{2})t} \right] \times \\ & \left[\hat{b}_0 + \hat{b}_0^\dagger + \hat{b}_r e^{-i(\Omega + \frac{\delta}{2})t} + \hat{b}_b e^{-i(\Omega - \frac{\delta}{2})t} + \hat{b}_r^\dagger e^{i(\Omega + \frac{\delta}{2})t} + \hat{b}_b^\dagger e^{i(\Omega - \frac{\delta}{2})t} \right]. \end{aligned} \quad (9)$$

This will yield the further operator equations as

$$\begin{aligned} \frac{\kappa}{2ig_0} \hat{a}_0 &= \hat{a}_0 (\hat{b}_0 + \hat{b}_0^\dagger) + \hat{a}_b \hat{b}_r^\dagger + \hat{a}_r \hat{b}_r, \\ \left[\frac{i(-\Omega + \frac{\delta}{2}) + \frac{\kappa}{2}}{ig_0} \right] \hat{a}_b &= \hat{a}_b (\hat{b}_0 + \hat{b}_0^\dagger) + \hat{a}_0 \hat{b}_b, \\ \left[\frac{i(\Omega + \frac{\delta}{2}) + \frac{\kappa}{2}}{ig_0} \right] \hat{a}_r &= \hat{a}_r (\hat{b}_0 + \hat{b}_0^\dagger) + \hat{a}_0 \hat{b}_r^\dagger. \end{aligned} \quad (10)$$

Now, substituting whatever we have in hand in the second equation of (10), and taking expectation values

at the end, we obtain a key algebraic equation in terms of δ as

$$i \left(-\Omega + \frac{1}{2}\delta \right) + \frac{1}{2}\kappa = ig_0(b_0 + b_0^*) + ig_0\sqrt{\bar{n}} \frac{2ig_0\sqrt{\bar{n}}}{i\delta + \Gamma}. \quad (11)$$

Rearrangement of the above gives rise to the equation

$$\delta^2 + [-i2\Omega + \gamma + 2g_0x_0]\delta + [(2\Omega - i\kappa)\Gamma - 4g_0^2\bar{n} + 2i\Gamma g_0x_0] = 0, \quad (12)$$

in which $x_0 = b_0 + b_0^*$ and $\gamma = \kappa + \Gamma$ is the total optomechanical decay rate [14, 16].

This approximate nature of this equation will yield complex values for δ the imaginary value of which has to be discarded. Furthermore, it leaves room to ignore the the square terms δ^2 , to admit the solution

$$\delta = \Re \left[\frac{(2\Omega - i\kappa)\Gamma - 4g_0^2\bar{n} + 2i\Gamma g_0x_0}{\gamma - 2i\Omega + 2g_0x_0} \right]. \quad (13)$$

This solution can be put into the more convenient form using (4) and further simplification as

$$\begin{aligned} \delta(\bar{n}) &= \Re \left[\frac{A + B\bar{n}}{C - iD\bar{n}} \right] \\ &= \frac{\Re[AC^*] + (B\Re[C] + \Im[A]D)\bar{n}}{|C|^2 - 2\Im[C]D\bar{n} + D^2\bar{n}^2} \\ &= \frac{[2\Gamma\Omega(\kappa + \gamma)] + (B\gamma - \kappa\Gamma D)\bar{n}}{|C|^2 - 4\Omega D\bar{n} + D^2\bar{n}^2}, \end{aligned} \quad (14)$$

where

$$\begin{aligned} A &= \Gamma(2\Omega - i\kappa), \\ B &= \frac{4g_0^2(\Omega - \frac{1}{2}\Gamma)^2}{\Omega^2 + \frac{1}{4}\Gamma^2} = B^*, \\ C &= \gamma - 2i\Omega, \\ D &= \frac{4g_0^2\Omega}{\Omega^2 + \frac{1}{4}\Gamma^2} = D^*. \end{aligned} \quad (15)$$

The expression (14) obtained for the side-band inequivalence has interesting properties at the limits of zero and infinite intracavity photon number. We may obtain here after some simplification easily the limiting expressions

$$\begin{aligned} \lim_{\bar{n} \rightarrow \infty} \delta(\bar{n}) &= 0, \\ \lim_{\bar{n} \rightarrow 0} \delta(\bar{n}) &= \frac{2\Gamma\theta\Omega}{4\Omega^2 + \gamma^2} \approx 0, \end{aligned} \quad (16)$$

with $\theta = \kappa + \gamma$, while noting that $\Gamma \ll \Omega$ and also for a side-band resolved cavity $\kappa \ll \Omega$, together which we have $\kappa < \gamma < \theta \ll \Omega$.

One should take into account the fact that for Doppler cavities, side-bands normally resolve well enough for a decisive measurement [18], and the concept of side-band inequivalence is only practically meaningful for side-band

resolved cavities. Therefore, the following approximations are valid

$$\begin{aligned} A &\approx 2\Gamma\Omega, \\ B &\approx 4g_0^2, \\ C &\approx -2i\Omega, \\ D &\approx \frac{4g_0^2}{\Omega}, \\ \delta(\bar{n}) &\approx \frac{\frac{1}{2}\Gamma\Omega^3\theta + g_0^2\Omega(\gamma\Omega - \kappa\Gamma)\bar{n}}{\gamma^2 + (\Omega^2 - 2g_0^2\bar{n})^2} \\ &\approx \frac{\frac{1}{2}\Gamma\Omega^3\theta + g_0^2\gamma\Omega^2\bar{n}}{\gamma^2 + (\Omega^2 - 2g_0^2\bar{n})^2}. \end{aligned} \quad (17)$$

As long as satisfies $\bar{n} \ll 2|\Im[C]|/D = \Omega^2/g_0^2$, then second order term \bar{n}^2 in the denominator of (15) is negligible and can be ignored. Under this regime, the side-band inequivalence varies almost linearly with \bar{n} as

$$\begin{aligned} \delta(\bar{n}) &\approx \frac{2\Gamma\theta\Omega}{4\Omega^2 + \gamma^2} + \frac{(B\gamma - \kappa\Gamma D)|C|^2 + 8\Omega^2\Gamma\theta D}{|C|^4}\bar{n} \\ &\approx \frac{g_0^2\gamma}{\Omega^2}\bar{n}. \end{aligned} \quad (18)$$

This result also behaves well in reasonable agreement with the expression obtained earlier for the side-band inequivalence [14] given as $\delta \approx g_0^2/\Omega$. The difference is within a fraction given by $\gamma/\Omega < 1$ which is typically less than unity.

The first immediate conclusion which can be obtained from (18) is that the side-band inequivalence δ is always positive, meaning that the detuning frequency of red-sideband should be always a bit larger in magnitude than the blue-sideband. This also agrees with the previous findings of higher-order operator algebra [14].

Another very important result which can be drawn from the above discussions, is marking the boundaries of linear, weakly nonlinear, and strongly nonlinear interaction regimes in quantum optomechanics. This follows by normalizing δ with respect to the mechanical frequency Ω first.

The linear regime is easily given by $\bar{n} < \Omega^2/g_0^2$, where intracavity photon number is essentially too low to cause any appreciable side-band inequivalence.

The weakly nonlinear regimes is next given by $\Omega^2/g_0^2 < \bar{n} < \Omega^3/g_0^2\gamma$, where the side-band inequivalence increases almost linearly.

The stongly nonlinear regime at larger intracavity photon numbers satisfying $\bar{n} > \Omega^3/g_0^2\gamma$ will push the system into strongly nonlinear regime where the side-band inequivalence quickly start to fade away.

The unique mathematical form of (14) which is composed of a first- and second-order polynomials in terms of \bar{n} respectively, offers a clear maximum at a certain optimum intracavity photon number \bar{n}_{\max} . To do this, let us first define the dimensionless constants $\alpha = 2g_0^2\gamma/\Gamma\Omega\theta$

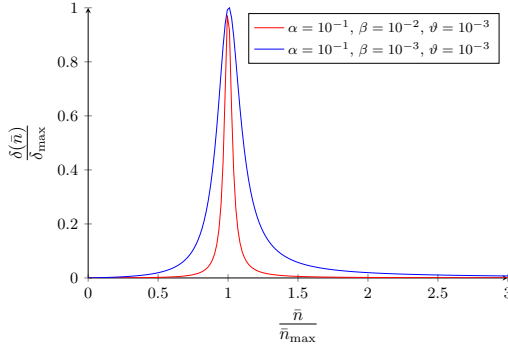


FIG. 1. Variation of side-band inequivalence around the maximum point in terms of various settings of parameters.

and $\beta = 2g_0^2/\Omega^2$, $\vartheta = \gamma/\Omega$, and $\psi = \Gamma\theta/2\Omega^2$. Then, the side-band inequivalence (17) can be rewritten as

$$\delta(\bar{n}) = \Omega\psi \frac{1 + \alpha\bar{n}}{\vartheta^2 + (1 - \beta\bar{n})^2}. \quad (19)$$

This offers the optimum intracavity photon number as

$$\bar{n}_{\max} = \frac{\sqrt{(\alpha + \beta)^2 + \alpha^2\vartheta}}{\alpha\beta} - \frac{1}{\alpha} \approx \frac{1}{\beta} = \frac{\Omega^2}{2g_0^2}, \quad (20)$$

and thus the maximum attainable side-band inequivalence as

$$\delta_{\max} = \delta(\bar{n}_{\max}) \approx \Omega\psi \frac{\alpha\beta}{\vartheta} = \frac{2g_0^4}{\Omega^3}. \quad (21)$$

Some further simplification and noting the fact that $\Omega \gg \Gamma\theta/\gamma$ or $\alpha \gg \beta$ and $\vartheta \ll 1$, we conclude that the maximum practically measureable side-band inequivalence must be simply given by $\delta_{\max} = 2g_0^4/\Omega^3$ at the optimum intracavity photon number $\bar{n}_{\max} = \Omega^2/2g_0^2$. This should fall at the onset of weakly nonlinear regime. In Fig. 1, variation of side-band inequivalence versus intracavity photon number and in terms of different settings for input parameters $\{\alpha, \beta, \vartheta\}$ is illustrated.

It is easy to verify that the side-band inequivalence does not violate the two fundamental symmetries of the nature. Here, both the time-reversal symmetry as well as the conservation of energy are preserved. The energy of scattered red- and blue- photons $\hbar\omega \mp \hbar\Omega$ is normally expected to be within the energy of one phonon $\hbar\Omega$ where ω is the angular frequency of incident electromagnetic radiation. Per every annihilated photon, exactly one phonon is either annihilated, giving rise to a blue-shifted photon, or one phonon is created, giving rise to a red-shifted photon.

However, not all photons and not all phonons are having exactly the same energies. This is permissible by the non-vanishing mechanical $\Gamma > 0$ and optical linewidths $\kappa > 0$ of the cavity. One should expect that once these two quantities vanish, the side-band inequivalence

is gone. This expectation is actually correct, and is met by the relation for the maximum observable side-band inequivalence δ_{\max} . Hence, basically it should be not contradictory to have a possible non-zero side-band inequivalence.

With regard to the time-reversal symmetry, one must take notice of the fact that all optical frequencies are physically positive, since we first must move back out of the rotating reference frame. For instance, the blue- and red-scattered photons have frequencies given by $\omega_b = \omega_c + \Omega - \frac{1}{2}\delta$ and $\omega_r = \omega_c - \Omega - \frac{1}{2}\delta$. Therefore, blue and red processes are not time-reversed processes of each other, as they both stay on the positive frequency axis. Negative frequency images corresponding to both processes do however exist and exactly satisfy the time-reversal symmetry.

Finally, it is easy to see that the same nonlinear symmetry breaking can lead to asymmetry in the particle pair production, which can be considered as the dual of optomechanical process [20, 21]. In order to observe this fact, consider an optomechanical system with a mechanical frequency roughly double the optical frequency $\Omega \approx 2\omega$. If the mechanics is driven strong enough at the frequency Ω , then the effective interaction Hamiltonian will be simply $\mathbb{H}_{\text{eff}} = i\hbar g(\hat{a}^\dagger \hat{a}^\dagger \hat{b} - \hat{a} \hat{a} \hat{b}^\dagger)$, where a phonon with energy $\hbar\Omega$ dissociates into two photons with energies $\hbar(\omega \pm \delta)$ where δ represents the corresponding symmetry breaking in pair frequencies caused by side-band inequivalence.

We presented a complete analysis of side-band inequivalence in quantum optomechanics, and showed it undergoes a maximum and obtained closed-form expressions for optimum intracavity photon number as well as maximum attainable side-band inequivalence. We classified the operation into the linear, weakly nonlinear, and strongly nonlinear regimes, in which the behavior of system is markedly different. The results of this investigation can provide the accuracy constraints as well as necessary experimental set up to resolve the elusive side-band inequivalence.

* sina.khorasani@ieee.org

- [1] M. Aspelmeyer, T. J. Kippenberg and F. Marquardt, "Cavity optomechanics," *Rev. Mod. Phys.* **86**, 1391–1452 (2014).
- [2] T. J. Kippenberg and K. J. Vahala, "Cavity optomechanics: back-action at the mesoscale," *Science* **321**, 1172–1176 (2008).
- [3] M. Aspelmeyer, T. Kippenberg, and F. Marquardt, *Cavity Optomechanics: Nano- and Micromechanical Resonators Interacting with Light* (Springer: Berlin, 2014).
- [4] P. Meystre, "A short walk through quantum optomechanics," *Ann. Phys.* **525**, 215–233 (2013).
- [5] W. P. Bowen, and G. J. Milburn, *Quantum Optomechanics* (CRC Press: Boca Raton, 2016).

- [6] W.-J. Gu, Z. Yi, L.-H. Sun, and Y. Yan, "Enhanced quadratic nonlinearity with parametric amplifications," *J. Opt. Soc. Am. B* **35** 652–657 (2018).
- [7] J.-S. Zhang, and A.-X. Chen, "Enhancing quadratic optomechanical coupling via nonlinear medium and lasers," arxiv, 1810.13052 (2018).
- [8] M. Hossein-Zadeh, and K. J. Vahala, "Observation of optical spring effect in a microtoroidal optomechanical resonator," *Opt. Lett.* **32**, 1611–1613 (2007).
- [9] K. Huang, and M. Hossein-Zadeh, "Direct stabilization of optomechanical oscillators," *Opt. Lett.* **42**, 1946–1949 (2017).
- [10] T. P. Purdy, P.-L. Yu, N. S. Kampel, R. W. Peterson, K. Cicak, R. W. Simmonds, and C. A. Regal, "Optomechanical Raman-ratio thermometry," *Phys. Rev. A* **92**, 031802(R) (2015).
- [11] T.P. Purdy, K. E. Grutter, K. Srinivasan, and J. M. Taylor, "Quantum correlations from a room-temperature optomechanical cavity," *Science* **356**, 1265–1268 (2017).
- [12] F. Marquardt, J. P. Chen, A. A. Clerk, and S. M. Girvin, "Quantum Theory of Cavity-Assisted Sideband Cooling of Mechanical Motion," *Phys. Rev. Lett.* **99**, 093902 (2007).
- [13] I. Wilson-Rae, N. Nooshi, W. Zwerger, and T. J. Kippenberg, "Theory of Ground State Cooling of a Mechanical Oscillator Using Dynamical Backaction," *Phys. Rev. Lett.* **99**, 093901 (2007).
- [14] S. Khorasani, "Method of Higher-order Operators for Quantum Optomechanics," *Sci. Rep.* **8**, 11566 (2018).
- [15] S. Khorasani, "Higher-Order Interactions in Quantum Optomechanics: Revisiting Theoretical Foundations," *Appl. Sci.* **7**, 656 (2017).
- [16] S. Khorasani, "Higher-Order Interactions in Quantum Optomechanics: Analytical Solution of Nonlinearity," *Photonics* **4**, 48 (2017).
- [17] S. Khorasani, "Higher-Order Interactions in Quantum Optomechanics: Analysis of Quadratic Terms," *Sci. Rep.* **8**, 16676 (2018).
- [18] S. Khorasani, "Momentum-field Interactions Beyond Standard Quadratic Optomechanics," in *Quantum Mechanics: Theory, Analysis and Applications*, A. I. Arbab, ed. (Nova Science Publishers, New York, 2018), Chapter 1, pp. 1–17.
- [19] S. Khorasani and B. Cabon, "Theory of optimal mixing in directly modulated laser diodes," *Scientia Iranica* **16**, 157–162 (2009).
- [20] O. Di Stefano, A. Settineri, V. Macrì, A. Ridolfo, R. Stassi, A. F. Kockum, S. Savasta, and F. Nori, "Interaction of Mechanical Oscillators Mediated by the Exchange of Virtual Photon Pairs," arxiv, 1712.00121 (2017).
- [21] E. Jansen, J. D. P. Machado, and Y. M. Blanter, "Realization of the degenerate parametric oscillator in electromechanical systems," arxiv, 1811.01605 (2018).